

Significant Reduction of Electronic Correlations upon Isovalent Ru Substitution of BaFe_2As_2

V. Brouet,¹ F. Rullier-Albenque,² M. Marsi,¹ B. Mansart,¹ M. Aichhorn,³ S. Biermann,³ J. Faure,^{4,5} L. Perfetti,⁵
A. Taleb-Ibrahimi,⁶ P. Le Fèvre,⁶ F. Bertran,⁶ A. Forget,² and D. Colson²

¹Laboratoire de Physique des Solides, Université Paris Sud, CNRS-UMR8502, 91405 Orsay, France

²Service de Physique de l'Etat Condensé, CEA Saclay, CNRS-URA2464, 91191 Gif-sur-Yvette, France

³Centre de Physique Théorique, Ecole Polytechnique, CNRS, 91128 Palaiseau, France

⁴Laboratoire d'Optique Appliquée, ENSTA, Ecole Polytechnique, CNRS-UMR7639, 91761 Palaiseau, France

⁵Laboratoire des Solides Irradiés, Ecole Polytechnique, CNRS-CEA/DSM, 91128 Palaiseau, France

⁶Synchrotron SOLEIL, UR1 CNRS, Saint-Aubin-BP48, 91192 Gif-sur-Yvette, France

(Received 25 February 2010; published 17 August 2010)

We investigate $\text{Ba}(\text{Fe}_{0.65}\text{Ru}_{0.35})_2\text{As}_2$, a compound in which superconductivity appears at the expense of magnetism, by transport measurements and angle resolved photoemission spectroscopy. By resolving the different Fermi surface pockets and deducing from their volumes the number of hole and electron carriers, we show that Ru induces neither hole nor electron doping. However, the Fermi surface pockets are about twice larger than in BaFe_2As_2 . A change of sign of the Hall coefficient with decreasing temperature evidences the contribution of both carriers to the transport. Fermi velocities increase significantly with respect to BaFe_2As_2 , suggesting a reduction of correlation effects.

DOI: 10.1103/PhysRevLett.105.087001

PACS numbers: 74.70.Xa, 71.27.+a, 74.25.F-, 74.25.Jb

A key similarity between iron pnictides (FePn) and cuprate superconductors is the proximity of magnetic and superconducting phases in their phase diagrams. BaFe_2As_2 is, for example, a semimetal with the same number of hole and electron carriers (in the following, we refer to this situation as “undoped”) and it undergoes a spin density wave (SDW) transition below 139 K [1]. However, whereas superconductivity is only observed in doped cuprate superconductors, there are a number of ways to induce it in FePn. In the BaFe_2As_2 family, it can be obtained through hole [2] or electron [3] doping, but also by applying pressure [4] or through isovalent substitutions, either P at the As site [5] or Ru at the Fe site [6]. It is likely that, whereas in cuprate superconductors the Mott insulating state has to be destroyed by doping before superconductivity may emerge, the itinerant nature of magnetism in BaFe_2As_2 makes it easier to switch to superconductivity. In this respect, FePn may be closer to heavy fermion systems [7], although they have much higher superconducting temperatures. Understanding such evolutions should give crucial information about the role of correlations and magnetism in the formation of the superconducting state.

Distressingly, very little information is available so far about the changes of the electronic structure leading to superconductivity in undoped compounds. It is not even established whether substitutions or pressure do or do not induce an effective doping. Particularly in the case of Ru/Fe substitutions, the possible formation of Ru^{4+} and Ru^{5+} (instead of a valence 2+ for Fe in the FeAs slab) could result in electron doping [8]. The first study of these compounds [6] in fact concluded that these systems were electron doped. On the contrary, a density functional theory calculation [8] predicts these systems to behave as coherent alloys, with an increased bandwidth, due to the

larger spatial extension of the Ru 4d orbitals. This larger bandwidth would lower the density of states at the Fermi level $n(E_F)$, and this may be the reason for the destabilization of the magnetic state. Similarly, changes of the structure under pressure or P/As substitution are under scrutiny to explain the appearance of superconductivity. Especially, it is known that the band structure is extremely sensitive to the Fe-As-Fe bond angle [9], which changes in all these different cases [10,11]. Clearly, direct experimental determination of the band structure in undoped superconductors is highly desirable to go further.

We present here a detailed investigation of $\text{Ba}(\text{Fe}_{0.65}\text{Ru}_{0.35})_2\text{As}_2$ (abbreviated in the following as $\text{BaFeRu}_{0.35}\text{As}$), a compound that is nonmagnetic and superconducting at 19.5 K. In contrast to BaFe_2As_2 , where the Hall coefficient R_H is always negative [12], R_H becomes positive here below 115 K, indicating a larger mobility of holes in $\text{BaFeRu}_{0.35}\text{As}$. By angle resolved photoemission spectroscopy (ARPES), we detect well-defined hole and electron bands, evidencing a homogeneous electronic structure and no strong disorder associated with Ru substitutions. The structure and nesting properties of the Fermi surface (FS) are similar to that of other compounds of this family [13–20], suggesting identical orbital origin for the different pockets. However, the electronic structure is strongly modified compared to BaFe_2As_2 : The number of both carriers (holes and electrons) has doubled and the Fermi velocities (v_F) have increased by a factor nearly 3. No similar tendency was observed under hole or electron doping, for which a simple rigid band filling picture applies well [13,17]. These changes largely exceed those expected in band structure calculations we performed for BaFe_2As_2 and BaFeRuAs_2 . We conclude that there is a substantial reduction of the

band renormalization upon Ru substitution, hence of correlation effects. The consequences of this situation for the competition between magnetism and superconductivity will be interesting to explore.

We have synthesized single crystals of $\text{Ba}(\text{Fe}_{1-x}\text{Ru}_x)_2\text{As}_2$ with sizes up to $0.5 \times 0.4 \times 0.02 \text{ mm}^3$, using a self-flux method [21]. We find that the a lattice parameter increases slightly with x , whereas c decreases, in agreement with Ref. [6]. For $x = 0.35$, $a = 4.0344(5) \text{ \AA}$, and $c = 12.760(3) \text{ \AA}$, which means that the Fe-As-Fe bond angle increases from 111.18° to 113.73° . Figure 1 shows that, at $x = 0.35$, corresponding approximately to optimal doping [21], the resistivity does not exhibit any sign of the SDW transition anymore and a superconducting state is stabilized under 19.5 K. Moreover, Hall effect measurements performed in the van der Pauw configuration in magnetic fields up to 14 T show that the Hall coefficient, which is negative at high temperature, becomes positive below 115 K. This behavior is very different from that observed in undoped and Co-doped BaFe_2As_2 , where R_H just decreases with temperature [12]. It is also different from that reported previously for polycrystalline samples of $\text{Ba}(\text{Fe}_{1-x}\text{Ru}_x)_2\text{As}_2$ [6], where R_H was found negative. This was interpreted as a sign of electron doping induced by Ru, but the present result in single crystals casts doubts on this conclusion. In a two band model, our positive R_H at low temperatures indicates that the mobility of holes overcomes the one of electrons in this limit. This implies that some scattering processes responsible for the low mobility of holes in BaFe_2As_2 are considerably reduced by the introduction of Ru. A complete analysis of the transport properties as a function of Ru doping is reported elsewhere [21].

Investigation of the electronic structure by ARPES clarifies the situation. Experiments were carried out at the CASSIOPEE beam line of the SOLEIL synchrotron. The photon energy was tuned between 35 and 100 eV and the polarization of the light was linear, either in the plane of incidence (named hereafter LHP for linear horizontal po-

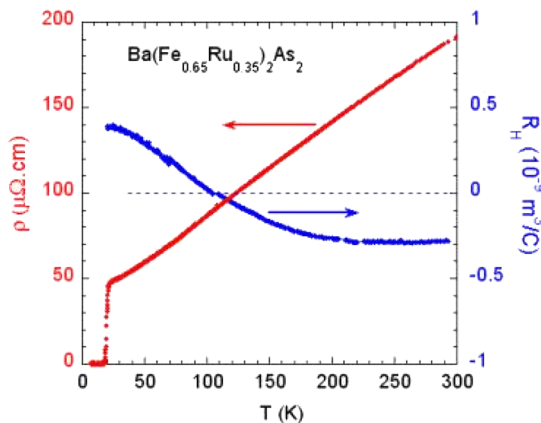


FIG. 1 (color online). Temperature dependence of the in-plane resistivity (left) and of the Hall coefficient R_H (right) in $\text{BaFeRu}_{0.35}\text{As}$.

larization) or perpendicularly to it (linear vertical polarization, LVP). Figure 2(a) presents the FS measured at 20 K and $k_z = \pi/c'$ (k_z is the direction perpendicular to the FeAs slab, it is quoted modulo $2\pi/c'$, where $c' = c/2$ is the distance between two FeAs slabs. It is fixed by the photon energy $h\nu$, through $k_z = 0.512\sqrt{h\nu - W + V_0}$, with $V_0 \approx 14 \text{ eV}$ in these compounds, see Refs. [17,18]). The FS structure is basically similar to that of BaFe_2As_2 , either pure or substituted with K (hole doping) or Co (electron doping) [13,14,17,22]. Two different circular hole pockets are present at the Brillouin zone (BZ) center Z [called hereafter α (inner red circle) and β (outer blue circle), the sizes of the circles were determined from Fig. 3]. Doubly degenerate electron pockets are found at the BZ corners X (black circle, see also Fig. 4). Figure 2(b) further shows that, as in BaFe_2As_2 [17–19], the sizes of the hole pockets appear strongly dependent on the photon energy, indicating substantial k_z dispersion (see supplementary information [23] for more details). The similar ratio and photon energy dependence of the two hole bands suggest that they are formed by the same orbitals, possibly with slightly stronger 3D effects in $\text{BaFeRu}_{0.35}\text{As}$. On the contrary, the electron pockets do not exhibit strong k_z dependence, although they are quite sensitive to experimental conditions (see Fig. 4). This is again similar to other FePn [17,19]. Note that, at first sight, the electron pockets would nest rather well into the inner hole pocket, if translated by $(\pi/a, \pi/a)$. The suppression of the SDW state then cannot be simply attributed to a worse FS nesting. Rather good nesting was also found in other FePn superconductors [13,16].

A major difference between these FS, however, is that the sizes of the hole pockets are much larger in $\text{BaFeRu}_{0.35}\text{As}$ than in BaFe_2As_2 . As the volume of the pockets is simply proportional to the number of holes or

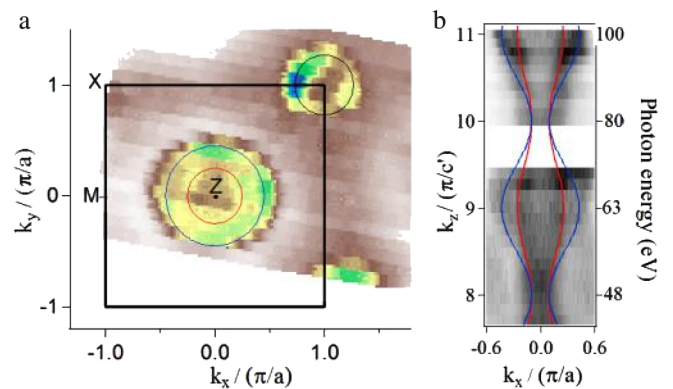


FIG. 2 (color online). (a) Fermi surface of $\text{BaFeRu}_{0.35}\text{As}$ at 20 K, with 100 eV photon energy (i.e., $k_z = 11\pi/c'$) and LHP. Spectral weight is integrated in a 10 meV window. Black square is the BZ of the 3D unit cell. Circles indicate the hole and electron pockets, as determined in the text. (b) Spectral intensity at E_F measured along k_x as a function of photon energy (right) or, equivalently, of k_z (left). Lines are cosine dispersion with k_z periodicity for the two hole pockets (see [23]).

electrons they contain, this is important information to consider. The diameter of the hole pockets can be accurately determined by the crossing of the hole bands with E_F . At $k_z = \pi/c'$, Fig. 3(d) indicates $k_F^\alpha = 0.25\pi/a$ and $k_F^\beta = 0.42\pi/a$ for BaFeRu_{0.35}As. This is almost twice larger than in BaFe₂As₂ [$k_F^\alpha = 0.14\pi/a$ and $k_F^\beta = 0.28\pi/a$ in Fig. 3(c)] and rather resembles the hole-doped Ba_{0.6}K_{0.4}Fe₂As₂ ($k_F^\alpha = 0.22\pi/a$ and $k_F^\beta = 0.43\pi/a$ [13]). Integrating the volume of the hole pockets over k_z using the contours shown in Fig. 2(b) (see [23] for details), we estimate they contain $n_h \approx 0.11$ holes/Fe. If BaFeRu_{0.35}As is undoped, one expects $n_h = n_{el}$, hence $k_F^{el} = 0.26\pi/a$ for two circular and degenerate electron pockets. This is indicated as a black circle in Fig. 2(a) and agrees very well with the actual size of the electron pocket. We therefore conclude that BaFeRu_{0.35}As is a compensated semimetal with $n = n_h = n_{el} \approx 0.11$ carriers/Fe.

This number of carriers is significantly larger than the value we estimated in BaFe₂As₂ $n = 0.06 \pm 0.02$ with a similar reasoning [17]. This leads to the very different contributions of holes and electrons in the transport properties of these two compounds observed in Fig. 1 [21]. Ortenzi *et al.* proposed that a reduced number of carriers compared to theoretical estimates ($n = 0.15$ in BaFe₂As₂ [24]) could be due to interband interactions [25]. This may then be a sign of different band interactions, see below.

The strong difference between the two electronic structures is further revealed by the comparison of their band dispersions. Figure 3 compares the dispersions at photon energies equivalent to $k_z = \pi/c'$, where the bands are most clearly separated (data in BaFe₂As₂ are shown at 150 K to avoid complications due to the magnetic phase). In BaFeRu_{0.35}As, the dispersions are clearly much steeper, they are almost parallel and a linear fit yields $v_F^\alpha =$

1.16 eV \AA and $v_F^\beta = 0.89 \text{ eV \AA}$. In BaFe₂As₂, the bands are more rounded and a linear fit near the Fermi level yields $v_F^\alpha = 0.43 \text{ eV \AA}$ and $v_F^\beta = 0.32 \text{ eV \AA}$, a factor 2.75 smaller. Although v_F formally depends on k_F ($v_F = \hbar k_F/m^*$), this difference is not due to the different k_F : the slope of the dispersions in BaFe₂As₂ would be nearly the same if measured at -0.03 eV [dotted line in Fig. 3(b)], where the crossings occur at values close to k_F in BaFeRu_{0.35}As. Also, in Ba_{0.6}K_{0.4}Fe₂As₂, where there is almost the same number of holes as in BaFeRu_{0.35}As, the dispersions are still very different, $v_F^\alpha = 0.5 \text{ eV \AA}$ and $v_F^\beta = 0.22 \text{ eV \AA}$ [13]. Therefore, there is a strong intrinsic increase of v_F in BaFeRu_{0.35}As.

To understand whether this increase is due mainly to changes in the band structure or to a different renormalization of the band structure, we performed electronic structure calculations within the local density approximation, using the WIEN2K package [26]. For BaFe₂As₂, we considered the tetragonal structure with cell parameters taken from [1]. The substitution by Ru has been studied for BaFeRuAs₂, where one of the two Fe atoms in the unit cell has been replaced by Ru, and with cell parameters reported here for BaFeRu_{0.35}As. Although this composition is slightly larger than the one studied here ($x = 0.5$ instead of $x = 0.35$), this gives a first idea of the qualitative evolution. In Figs. 3(c) and 3(d), these calculations are compared to the dispersions determined experimentally. For BaFe₂As₂, a renormalization by a factor about 3 would be needed to align the dispersions, in agreement with previous studies [22] and theoretical expectations of correlation strength in FePn [27]. On the contrary, it would be negligible for BaFeRu_{0.35}As. The increase of v_F is then not primarily driven by changes in the band structure, but by significantly smaller correlation effects.

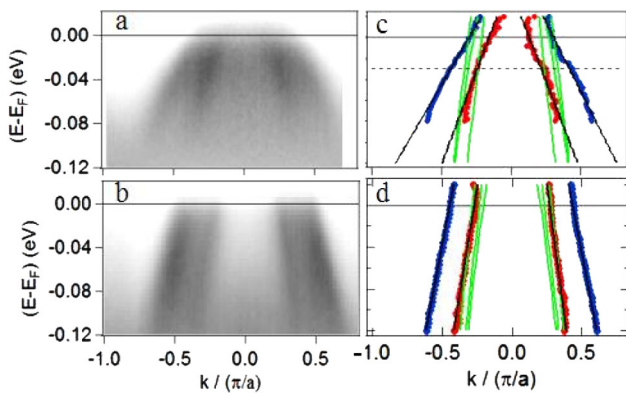


FIG. 3 (color online). Hole pockets: (a) ARPES intensity plot measured around Z in BaFe₂As₂, at 150 K, with 34 eV photon energy ($k_z = 7\pi/c'$) and LHP. (b) Same for BaFeRu_{0.35}As at 20 K, with 100 eV photon energy and LHP. (c) and (d) Points: Dispersions extracted by a 4 Lorentzian fit of the momentum distribution curves (MDC) of the left images, with linear fits. Thick green lines are the calculated dispersions along ZM for the three hole bands (see text).

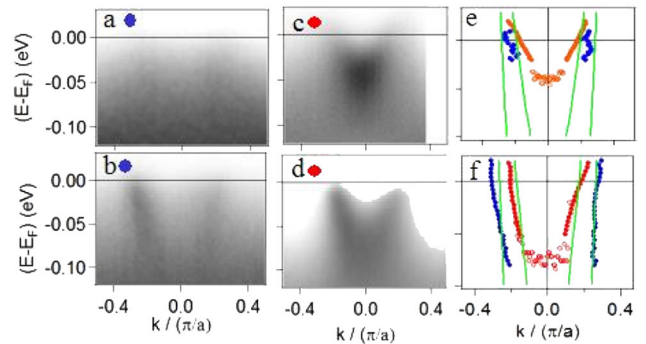


FIG. 4 (color online). Electron pockets (the center was taken as $k = 0$): (a) ARPES intensity plot measured in BaFe₂As₂ at 150 K, with 92 eV photon energy and LHP, (c) same with 34 eV and LVP. (b) Same in BaFeRu_{0.35}As at 20 K, with 100 eV photon energy and LHP, (d) same with 45 eV and LVP. (e) and (f) Dispersions of the left images extracted by a MDC fit. Bottom of the band (open circles) is defined as maximum of the energy-distribution curve, when possible. Thick green lines are dispersions obtained by band structure calculations (see text) for the two electron bands along ΓX .

Figure 3 further shows that the three hole bands should be shifted with respect to E_F to obtain a good agreement with experiment. These shifts should mostly enlarge the pockets in $\text{BaFeRu}_{0.35}\text{As}$ and shrink them in BaFe_2As_2 . This corresponds to the larger FS in the former compound we have already discussed, but further indicates that this change is not expected at the band structure level and should then be associated to correlations and/or different interband interactions [25]. These shifts are likely orbital sensitive and may also depend on k_z , so that orbital symmetries, 3D effects, exact dopings and structures, will be very important to consider to fully quantify the nature of these changes.

The behavior of the electron pockets presented in Fig. 4 is consistent with that of the holes. Band structure calculations [Figs. 4(e) and 4(f)] predict two electron bands, with quite different v_F for the inner and outer bands. These two bands are usually not clearly resolved experimentally, but we observed empirically that the contribution of the outer band is dominant for photon energy around 100 eV and LHP [Figs. 4(a) and 4(b)] and that of the inner band for lower photon energies and LVP [Figs. 4(c) and 4(d)]. Because the bands cannot be clearly separated, it is more difficult to compare v_F directly [28]. Nevertheless, the tendency of smaller renormalization for $\text{BaFeRu}_{0.35}\text{As}$ holds. We also observe that the bottom of the inner electron band seems to shift from 40 to 70 meV in $\text{BaFeRu}_{0.35}\text{As}$ [open circles in Figs. 4(c) and 4(f)], suggesting larger bandwidth, consistent with the larger Fermi velocities. Better separation of the two bands will be needed for more quantitative comparison.

Finally, we have established that the electronic structure is qualitatively similar in $\text{BaFeRu}_{0.35}\text{As}$ and BaFe_2As_2 , as far as the number of holes and electrons pockets, their 3D character and probably their main orbital origin is concerned. However, correlation effects appear strongly reduced in $\text{BaFeRu}_{0.35}\text{As}$ and, in fact, almost negligible compared to our calculations within local-density approximation. This can explain the increased mobility of holes in $\text{BaFeRu}_{0.35}\text{As}$ compared to BaFe_2As_2 revealed by Hall measurements. The bandwidth we calculate in BaFeRuAs_2 is substantially larger (~ 6 eV) than that of BaFe_2As_2 (~ 4 eV), similarly to [8], naturally leading to weaker correlations, even for comparable interactions. We attribute this to increased covalency effects of Ru ions compared to Fe. These different correlations strengths may have important consequences for the ordering of the different orbitals and finely tune the orbital weights at the FS. As the occupation of the different orbitals probably depends sensitively on the correlations, it is worth stressing that we simultaneously observe quite a different number of carriers compared to BaFe_2As_2 . The resulting electronic structure of this undoped FePn superconductor is then markedly different from that of doped FePn superconductors, despite their similar T_c . Interestingly, a de Haas–van Alphen investigation in $\text{BaFe}_2(\text{As}_{1-x}\text{P}_x)_2$ recently reported larger FS areas and lower effective mass upon P

substitution [29]. This suggests that the two effects are really linked and that this modification is characteristic of undoped superconductors. The delicate balance between the different orbitals may play a crucial role for stabilization of magnetism or superconductivity. Furthermore, this example shows that one can tune quite significantly the band structure and correlations in iron pnictides, revealing notably that the absolute number of carriers is probably an additional important parameter.

We thank H. Alloul, J. Bobroff, Y. Laplace, and A. Georges for discussions and P. Thuéry for help with structural measurements. M. A. acknowledges financial support from the Austrian Science Fund, project J2760.

-
- [1] M. Rotter *et al.*, *Phys. Rev. B* **78**, 020503(R) (2008).
 - [2] M. Rotter, M. Tegel, and D. Johrendt, *Phys. Rev. Lett.* **101**, 107006 (2008).
 - [3] A. S. Sefat *et al.*, *Phys. Rev. Lett.* **101**, 117004 (2008).
 - [4] P. L. Alireza *et al.*, *J. Phys. Condens. Matter* **21**, 012208 (2009).
 - [5] S. Jiang *et al.*, *J. Phys. Condens. Matter* **21**, 382203 (2009).
 - [6] S. Sharma *et al.*, *Phys. Rev. B* **81**, 174512 (2010).
 - [7] N. D. Mathur *et al.*, *Nature (London)* **394**, 39 (1998).
 - [8] L. Zhang and D. Singh, *Phys. Rev. B* **79**, 174530 (2009).
 - [9] V. Vildosola *et al.*, *Phys. Rev. B* **78**, 064518 (2008).
 - [10] S. A. J. Kimber *et al.*, *Nature Mater.* **8**, 471 (2009).
 - [11] J. Zhao *et al.*, *Nature Mater.* **7**, 953 (2008).
 - [12] F. Rullier-Albenque, D. Colson, A. Forget, and H. Alloul, *Phys. Rev. Lett.* **103**, 057001 (2009).
 - [13] H. Ding *et al.*, *Europhys. Lett.* **83**, 47001 (2008); H. Ding *et al.*, arXiv:0812.0534; Y. Xu *et al.*, arXiv:0905.4467.
 - [14] C. Liu *et al.*, *Phys. Rev. Lett.* **101**, 177005 (2008).
 - [15] M. Yi *et al.*, *Phys. Rev. B* **80**, 174510 (2009).
 - [16] K. Terashima *et al.*, *Proc. Natl. Acad. Sci. U.S.A.* **106**, 7330 (2009).
 - [17] V. Brouet *et al.*, *Phys. Rev. B* **80**, 165115 (2009).
 - [18] P. Vilmercati *et al.*, *Phys. Rev. B* **79**, 220503(R) (2009).
 - [19] W. Malaeb *et al.*, *J. Phys. Soc. Jpn.* **78**, 123706 (2009).
 - [20] S. Thirupathiah *et al.*, *Phys. Rev. B* **81**, 104512 (2010).
 - [21] F. Rullier-Albenque *et al.*, *Phys. Rev. B* **81**, 224503 (2010).
 - [22] M. Yi *et al.*, *Phys. Rev. B* **80**, 024515 (2009).
 - [23] See supplementary material at <http://link.aps.org/supplemental/10.1103/PhysRevLett.105.087001> for more details on 3D effects.
 - [24] G. Xu, H. Zhang, X. Du, and Z. Fang, *Europhys. Lett.* **84**, 67015 (2008).
 - [25] L. Ortenzi, E. Cappelluti, L. Benfatto, and L. Pietronero, *Phys. Rev. Lett.* **103**, 046404 (2009).
 - [26] P. Blaha *et al.*, *WIEN2K, An Augmented PlaneWave Plus Local Orbitals Program for Calculating Crystal Properties* (Techn. Universität Wien, Wien, Austria, 2002), ISBN 3-9501031-1-2.
 - [27] M. Aichhorn *et al.*, *Phys. Rev. B* **80**, 085101 (2009).
 - [28] Some asymmetry in the dispersion is likely due to a different combination of the two electron bands on the two sides.
 - [29] H. Shishido *et al.*, *Phys. Rev. Lett.* **104**, 057008 (2010).